Extreme midsummer rainfall event drives early onset cyanobacterial bloom

Megan L. Larsen[1], Helen M. Baulch[2], Sherry L. Schiff [3], Dana F. Simon[4], Sébastien Sauvé [4], and Jason J. Venkiteswaran[1*]

[1]*Department of Geography and Environmental Studies, Wilfrid Laurier University, 75 University West, Waterloo, Ontario Canada N2L 3C5*

[2]*School of Environment and Sustainability, Global Institute for Water Security, University of Saskatchewan, 323 Kirk Hall, 117 Science Place, Saskatoon Saskatchewan Canada, S7N 5C8*

[3]*Department of Earth and Environmental Sciences, University of Waterloo, 200 University Avenue West, Waterloo, Ontario Canada N2L 3G1*

[4] *Department of Chemistry, Université de Montréal, 2900 Édouard-Montpetit, Montréal, Quebec Canada H3C 3J7*

* corresponding author: jvenkiteswaran@wlu.ca

Abstract

The prevalence and increasing global distribution of cyanobacteria-dominated harmful algal blooms is strongly associated with changing climatic patterns and local biogeochemical and hydrological processes. Changes to precipitation frequency and intensity, as predicted by current climate models, are likely to alter bloom development and composition due to nutrient fluxes and water column mixing. However, few studies have directly documented the effects of precipitation events on cyanobacterial composition, biomass, and toxin production. In this study, we describe an early-initiated cyanobacterial bloom in Conestogo Lake, a eutrophic flood control reservoir located in southwestern Ontario, following heavy rainfall and subsequent flooding within the catchment. A surge in bioavailable phosphorus resulted in biomass increases of *Aphanizomenon flos-aquae* throughout the reservoir approximately 2 weeks post-flooding. Anabaenopeptin-A and three microcystin congeners (microcystin-LR, -YR, and -RR) were detected at varying levels across sites during the bloom period, which lasted between 3 - 5 weeks. In addition, each of the three sampled sites varied in physical and chemical properties throughout the sampling campaign suggesting different eco-zones within the reservoir that may be influenced by flow. Together, these findings indicate that water column mixing and phosphorus concentrations were the key drivers for the early cyanobacterial bloom in Conestogo Lake and further highlight the complex relationship and variability within reservoir systems. Therefore, effective management goals and mitigation strategies for bloom-related water quality impairment must be both responsive and adaptive to the complexity of drivers affecting blooms.

Key words: cyanobacterial bloom, harmful algal bloom, Ontario, reservoir, extreme rainfall

Introduction

Cyanobacteria are critical to the structure and function of aquatic communities (Reynolds 1984, Wetzel 2001). However, prolific cyanobacterial growth often negatively impacts ecosystems by reducing water quality and driving disruptions to aquatic food chains (Paerl 1988). Several bloom-forming species also synthesize an array of bioactive compounds that pose chronic and acute health risks to humans and animals through dermal contact, inhalation, and/or ingestion of contaminated waters (Chorus et al. 2000, Codd 2000, Carmichael 2001). Blooms and their associated bioactive metabolites also have economic consequences through potential losses in tourism, recreational activities, and water treatment upgrades (Bullerjahn et al. 2016).

The increased prevalence of cyanobacterial blooms has been historically attributed to increased anthropogenic eutrophication, with emphasis on the relative abundances, contributions, and impacts of nitrogen and phosphorus (Winter et al. 2012, Paerl and Otten 2013). Changing climatic conditions are also now strongly considered in significant drivers in bloom intensity and distribution (Paerl and Huisman 2009, O'Neil et al. 2012, Sukenik et al. 2015, Paerl et al. 2016). Many current climate models predict increasing regional temperatures likely resulting in warmer surface waters, increased thermal stratification, and water column stability that promote the growth of certain bloom-forming species (Jöhnk et al. 2008, Paerl and Huisman 2009). Precipitation frequency and intensity are also predicted to change, but less attention has been given to how these factors may influence bloom development and cyanobacterial biomass (Reichwaldt and Ghadouani 2012).

Increasing precipitation variability may impact external nutrient and sediment delivery to waterbodies, alter residence time and flushing, and reduce vertical stratification, which, in turn, may affect bloom development (Jacobsen and Simonsen 1993, Mitrovic et al. 2003, Wood et al.

66 2017). For example, Wood *et al.* (2017) reported decreased cyanobacterial biomass
67 following an extreme rainfall event that lead to water column cooling and destratification
68 in a shallow, eutrophic New Zealand lake. Intense precipitation, preceded or followed by
69 extensive drought may create episodic or pulsed nutrient loads potentially further
70 favoring cyanobacterial development (Bouvy et al. 2003, Reichwaldt and Ghadouani
71 2012). In addition to climatic factors, bloom development is also dependent on a suite of
72 site-specific characteristics including hydrology, lake geomorphology, catchment size,
73 and nutrient loading from internal and external sources. Thus, the sensitivity of each lake
74 to these drivers, including precipitation, will vary.

75 Cyanobacterial blooms are of particular concern for lake and reservoir managers
76 due to the potential for toxin production and impacts on water quality that may affect
77 ecosystem processes and the recreational uses of the water body (Chorus and Bartram
78 1999, Chorus et al. 2000). Cyanobacterial metabolites are both chemically variable and
79 bio-actively diverse (Carmichael 1997, Welker and Von Döhren 2006) with various
80 modes of cellular action that may cause superficial skin irritation at low exposures and
81 sickness or even death if ingested at high enough concentrations (Pouria et al. 1998,
82 Chorus et al. 2000, Carmichael et al. 2001, Carmichael 2001). Often, the recommended
83 course of action for recreational waterbodies is to limit activity in and exposure to bloom-
84 affected waters due to accidental ingestion and/or inhalation during recreational activities
85 (Backer et al. 2010). As an exemplar of precipitation driving cyanobacterial blooms, we
86 focus on Conestogo Lake (Ontario, Canada; Figure 1), a eutrophic flood-control and river
87 augmentation reservoir, which has experienced recurring, late-fall cyanobacterial blooms
88 dominated by *Aphanizomenon flos-aquae.* On 23 June 2017, the Upper Conestogo

89 watershed received a significant amount of rainfall (daily avg. 78 mm at Conestogo Dam) that
90 resulted in severe flooding. According to the GRCA, nearly 80-85% of the volume of Conestogo
91 Lake was flushed downstream during this 2-day event (Grand River Conservation Authority
92 2018). This event provided a unique opportunity to explore how intense rainfall affects the
93 phytoplankton community and cyanobacterial bloom development.
94

95 ## *Materials and methods*

96 **Study Site**

97 Conestogo Lake is located in southwestern Ontario, Canada and operated as a bottom-draw
98 reservoir (7.35 km^2) by the Grand River Conservation Authority (GRCA; Mapleton Township,
99 ON). Built in 1958, it primarily serves as a flood-control and down-stream flow augmentation
100 system while providing ancillary recreational benefits for fishing, boating, and ~ 400 summer
101 cottages. Spring melt from the Upper Conestogo River basin (566 km^2), a predominately
102 agricultural catchment (> 80 %, Figure 1, *left*) is captured in the reservoir through the end of
103 April and is used during the summer drawdown (*i.e.* augmentation) period from 01 May to 30
104 September to provide consistent downstream flow of the Conestogo and Grand Rivers. As a
105 result of the reservoir drawdown, mean lake depth varies throughout the season with the deepest
106 point always near the dam. Reservoir storage volume during the summer augmentation period
107 has historically ranged between 12.7 and 56.3 Mm^3 (59.3 Mm^3 max cap.) with an average drop
108 between 5 and 9 m in stage elevation.
109

110 **Sample collection and analysis**

111 Sampling at Conestogo Lake began on 21 Jun 2017 with physical and biological samples
112 collected from the center (CLC) site closest to the dam. Two additional sites in the east (CLE)
113 and west (CLW) arms of the reservoir were added on 05 Jul and 11 Jul, respectively, following
114 the flooding event to assess the potential differences between catchment inputs into the reservoir
115 (Figure 1). From each location we collected a suite of physical, chemical, and biological data
116 throughout the water column. Physical water column profiles were collected at 0.5 m increments
117 using an EXO2 sonde (YSI, Yellow Springs, OH) equipped with chlorophyll-a, pH, temperature,
118 and dissolved oxygen sensors. The Secchi disk transparency at each site was used to collect
119 samples for cyanobacterial toxin analysis described in further detail below. In addition, we
120 collected discrete samples from 2 m for water chemistry and phytoplankton taxonomy and
121 enumeration approximately once per week from 21 June 2017 to 17 August 2017.
122 Whole water samples were collected for total phosphorus (TP) and
123 phytoplankton enumeration. Subsamples were field-filtered using a 0.45 µm syringe
124 filter (Whatman) for soluble reactive phosphorus (SRP), total dissolved phosphorus
125 (TDP), ammonia (NH_4-N), nitrate (NO_3-N), total dissolved nitrogen (TDN), anions, and
126 cations. All samples were transported on ice, stored at -20 °C, and analyzed at the
127 Environmental Geochemistry Laboratory at the University of Waterloo (Waterloo, ON)
128 as per AHPA (1998; see Table S1 for instrument listing and detection limits).
129 Phytoplankton identification and enumeration were completed by D. Findlay
130 (Plankton-R-Us, Winnipeg, MB, http://www.plankton-r-us.ca) as per Findlay & Kling
131 (2003). Briefly, phytoplankton samples were collected in a dark bottle, preserved with
132 Lugol's solution, and stored at 4 °C until analysis. Ten-mL aliquots of Lugol's
133 preserved sample were gravity settled for 24 h and counted using a modified Ütermohl

technique (Nauwerk 1963) on an inverted microscope with phase contrast illumination. Cell counts were converted to wet weight biomass by approximating cell volume, which were obtained by measurements of up to 50 cells of an individual species and applying the geometric formula best fitted to the shape of the cell (Vollenweider 1968, Rott 1981). A specific gravity of 1 was assumed for cellular mass. All biomass estimates are expressed as mg/m^3 (D. Findlay, pers. communication).

Total (*i.e.*, intracellular and extracellular) cyanobacterial metabolite concentrations were determined from a 115 mL whole water sample calculated from the site-specific Secchi depth (2× Secchi depth) at each site. Each sample was collected in an amber NalgeneTM polyethylene terephthalate glycol (PETG) bottle to limit adsorption and overflow during freezing (Fisher reference: 322021-0125). All samples were stored at -20 °C until analysis at the University of Montreal (Montréal, QC). Samples were prepared and screened for each of seventeen cyanobacterial compounds (Table S2) as per Fayad *et al.* (2015) via on-line solid phase extraction ultra-high performance liquid chromatography high resolution mass spectrometry (SPE−UHPLC–HRMS) using standards purchased from Enzo Life Science, Abraxis, or Cyano Biotech GmbH. The limit of detection (LOD) and limit of quantification (LOQ) were calculated for every batch of samples. Only results that exceeded the LOQ were included in our analysis. Therefore, some samples may have had detectable, but unquantifiable toxin concentrations.

Environmental and dam-related data

Meteorological and other reservoir-related data for this study were obtained from the GRCA's online data portal (https://data.grandriver.ca/). Because GRCA data are provided under a provisional status, all GRCA data were passed through quality assurance and quality checking

157 metrics for outliers to ensure sound data structure before proceeding with analysis. Spatial data
158 were obtained from open source portals at the GRCA (bathymetry), the United States Geological
159 Society, Statistics Canada, and the Ontario Ministry of Natural Resources (land-use).
160
161 **Data analysis and statistics**
162 All data analysis was completed in R version 3.5.1 (R Core Team 2018). Water column profile
163 data derived from sonde measurements as well as the discrete chemical profiles were constructed
164 using a multilevel B-spline interpolation from the *MBA* package (Finley et al. 2017) and were
165 adjusted to reflect the reservoir stage elevation at the time of sampling. One sampling in the east
166 arm contained a high chlorophyll-a concentration that skewed the profiles for all other sites.
167 Therefore, we log transformed (base 10) the data to allow for better visual comparison.
168 Comparisons of chemical and physical data across sites were completed using principal
169 coordinates analysis (PCoA) with a Euclidean matrix on log-normalized data to account for
170 scaling differences in the dataset and tested for difference through time and by site using
171 permutational analysis of variance (PERMANOVA) with *adonis* in the *vegan* package
172 (Okasanen et al. 2016). Similarly, we tested for differences in the phytoplankton community
173 composition by biomass using PCoA with a Bray-Curtis dissimilarity matrix on log-transformed
174 data to account for rare species biomass in the community and tested for difference through time
175 and by site using PERMANOVA. Biomass and toxin trends were analyzed using repeated
176 measures ANOVA (RM-ANOVA) with a linear mixed effects model (*lme*) from the *nlme*
177 package (Pinheiro et al. 2018) where time was a fixed effect, sampling location as a random
178 effect, and the correlation matrix selected based on Akaike Information Criterion (AIC).
179 Relationships between cyanobacterial biomass and environmental drivers including surface

water temperature and phosphorus concentrations were also completed using RM-ANOVA. In addition, we tested for the correlation of biomass with toxin concentrations using Kendall's rho. All code used for this project are available on github at https://github.com/biogeochem/formbloom_conestogo_2017HAB.

Results

Flood event

The Upper Conestogo watershed received an intense rainfall event on 23-24 June 2017. This two-day event increased mean daily flow from 4.56 m^3/s to 219 m^3/s (max 521 m^3/s), increased the total reservoir volume by 3.5 Mm^3 (million cubic meters), and is estimated to have replaced ~80% of the reservoir volume (Grand River Conservation Authority 2018). Within several days, the reservoir storage and drawdown returned to engineered levels (Figure 1*b*-*e*). The sizable influx of water from the catchment during the flood event increased measurable phosphorus by the next sampling on 05 July 2017 between 1.9 to 33× within the water column at the center site but did not affect any measured nitrogen species (Figures 2 and S1).

Hydrology and Descriptive Limnological Characteristics

All measured forms of phosphorus increased in the water column following the severe rainfall event (Figure 2*a*, Tables 1 and S1). Epilimnetic concentrations declined throughout the sampling period while hypolimnetic concentrations, notably TDP and TP, increased between 12 July (DOY 193) and 26 July (207) across all three sites. All nitrogen species (Figure 2*b* and S1, Tables 1 and S1) were well mixed throughout the water column and gradually decreased throughout the sampling campaign.

Conestogo Lake was initially and only briefly thermally stratified at the center site on 21 June 2017. By 05 July (DOY 186), the lake was isothermal across the lake and remained isothermal throughout the rest of the summer augmentation period (Figure S2*a* and Table 1). Mean surface water temperatures (0 - 2 m) ranged from 21.2 to 25.5 °C. Subsequent flow from the catchment following the 23 July rainfall reduced the surface water temperatures in the east and center by approximately 2 °C from the previous sampling but did not affect the surface temperatures in the west arm or center sites. Dissolved oxygen (Figure S2*b*, Tables 1 and S1) at the surface was highest during peak biomass. Hypoxia developed in the hypolimnion at all three sampling locations just as bloom biomass started to increase. Epilimnetic (0 - 2 m) chemical (TDN, NO_3-N, DOC, SRP, TDP, TP, SO_4^{2-}, Mn, Ca^{2+}, K^+, Na^+, Mg^{2+}, F^-, Cl^-) and physical (surface temperature, dissolved oxygen, residence time) properties were significantly different between sites (PERMANOVA, $P = 0.013$) and changed over the course of the sampling period (PERMANOVA, $P = 0.001$; Figure S3).

Early onset of cyanobacterial bloom

Within two weeks of the flooding event, measurable increases in cyanobacterial biomass dominated (> 95%) by the filamentous nitrogen-fixer *Aphanizomenon flos-aquae* were detected in each of the sampling locations (Figure 3). Epilimnetic phytoplankton composition significantly changed over the course of the sampling campaign with assemblages in the west and center more similar than those in the east (Figure S4, PERMANOVA, site: $F = 2.22$, $P = 0.001$, time: $F = 2.69$, $P = 0.003$). While other phytoplankton groups were represented (Figure S5), cyanobacteria exceeded 50% of the phytoplankton community in the east and west arms

226 near 12 July and approximately a week later in the center. Total cyanobacterial biomass varied
227 across sites and was significantly affected by eplimnetic SRP, mean daily flow rates, and surface
228 water temperatures (RMANOVA, $F_{1,462} = 778.79$, $P < 0.0001$); the east arm contained the
229 highest measured biomass on 19 July (DOY 200, 10,900 mg/m^3, 4,500 cells/mL), which declined
230 following another rainfall event on 23 Jul 2017. The center and west arm biomass peaked near
231 25 Jul (DOY 206; center: 4,710 mg/m^3, west: 5,230 mg/m^3). Bloom duration, measured as the
232 period during which cyanobacterial biomass composed > 50% of the fractional biomass,
233 persisted between 26 and 34 days and occurred 4 to 6 weeks earlier than has been previously
234 documented by the GRCA (S. Cooke, pers. communication). The cyanobacterial fraction across
235 all sampling sites also included *Woronichinia compacta*, *Anabaena (Dolichospermum) flos-*
236 *aquae*, *Microcystis aeruginosa*, *Anabaena* (*Dolichospermum) crassa, Planktolyngbya limnetica,*
237 and *Pseudoanabaena sp.* (Figure 3*a*). *W. compacta* exhibited similar biomass trends to *A. flos-*
238 *aquae*, though at much smaller biomass levels; by 17 Aug, its biomass increased to 8% (193.8
239 mg/m^3), 13% (108.9 mg/m^3), and 18% (585.9 mg/m^3) of the cyanobacterial biomass in the west,
240 center, and east, respectively.
241
242 **Cyanotoxins were detectable at low concentration**s
243 Detectable anabaenopeptin-A (AP-A), microcystin-LR (MC-LR), -YR, and -RR were present in
244 90 % of the samples ($n = 19$) but were only quantifiable in 81 % ($n = 17$; Table 2). Total
245 microcystin concentration did not exceed 1.0 µg/L throughout the sampling season and were
246 comparable to previously measured concentrations during the summer months (Yakobowski
247 2008). Metabolite type and concentration varied through time, but not by site (RMANOVA,
248 toxin × time, $F_{3,60} = 9.90$, $P < 0.0001$; site $P > 0.05$). Quantifiable concentrations of all three

249 microcystins were present in the east arm, MC-LR and MC-YR in the center site, and only MC-
250 LR in the west. MC-LR was the dominant microcystin variant across all sites with the highest
251 quantified values in the east arm at peak *A. flos-aquae*, *M. aeruginosa*, and *P. limnetica* biomass
252 (Figure 3, Table 2). Further, MC-YR at the center did not correspond with the MC-LR peak
253 suggesting its possible origin in the east arm. AP-A was present at all sampling locations
254 throughout the bloom period, was the dominant metabolite at all sites by 25 July (DOY 206), and
255 had replaced all microcystin variants by the end of the sampling campaign. Toxin concentrations
256 were not significantly correlated with the biomass of any particular cyanobacterial species
257 (Kendall rho, $P > 0.05$).
258

259 ## *Discussion*

260 Conestogo Lake has experienced annual cyanobacterial blooms over the last decade, some of
261 which have resulted in the issuance of health advisories for recreational users and cottage owners
262 (S. Cooke, GRCA, pers. communication). The sequence of high external P loads following the
263 23 June 2017 flood event, warming surface waters in the weeks thereafter, and reduced flow into
264 the reservoir all appear to have set the conditions for an early onset cyanobacterial bloom.
265 Dominance by *Aphanizomenon flos-aquae* in Conestogo Lake (Yakobowski 2008) and across
266 other Ontario waterbodies (Winter et al. 2011) is consistent with previous reports despite the
267 high N concentrations; however, the occurrence of blooms in this region is typically reported
268 during the late summer. Based on anecdotal reports (S. Cooke, GRCA, pers. communication) and
269 sampling results from our 2018 campaign (Larsen *et al*. in prep.), cyanobacterial blooms in
270 Conestogo Lake typically occur in mid- to late-August and persist through September or early
271 October.

Global increases in extreme rainfall events are predicted to outpace changes in total precipitation under various climate models (Allen and Ingram 2002, IPCC 2007) suggesting that heavy rain and flooding events will become more common in the near future. Limited studies investigating such events on cyanobacterial bloom development have identified changes to flushing rates, water column mixing, and nutrient inputs from rainfall events as the main factors affecting cyanobacteria and phytoplankton communities (Bouvy et al. 2003, Reichwaldt and Ghadouani 2012). These effects may be further accentuated by prolonged dry-periods, which increase nutrient release from soils. In Conestogo Lake, heavy rainfall increased soluble and particulate P between 1.9 – 33 X and resulted in a marked increase of cyanobacterial biomass and eventually, community dominance within 2 weeks of the flood event. NO_3-N and TDN remained high throughout the summer but did not noticeably change as a result of flooding.

High intensity rainfall events have also documented instances of bloom collapse due to de-stratification, increased turbidity, dilution, and flushing (Jacobsen and Simonsen 1993, Jones and Poplawski 1998, Wood et al. 2017). These studies do not align with our flood period in Conestogo Lake where the water column was well mixed prior to the onset of the cyanobacterial bloom and further, the rainfall event occurred early in phytoplankton succession when the community was dominated by chlorophytes and chryptophytes. However, they are consistent with the reduced *A. flos-aquae* and *W. compacta* biomass in the shallow east arm after a ~10 mm rainfall event in late July and its subsequent flow reduced surface water temperatures in the east by ~1.5 °C. Though it did not lead to major changes in N or P concentrations, the increased flow into the reservoir likely mixed the water column, creating unfavorable conditions for continued *A. flos-aquae* biomass accumulation. We also noted spatial variation in in phytoplankton community structure and cyanobacterial biomass within the reservoir. Some of these differences

295 are likely attributable to bottom depth and the relationship to the dam, however, its more
296 likely that they are influenced by the hydrologic flows. The east arm is the source of
297 most, if not all, of the flow into the reservoir, hence the phytoplankton community is
298 more likely to be susceptible to flow from the Conestogo River. Together, these results
299 suggest that the timing of the rainfall event with regard to the phytoplankton community
300 succession as well as the hydrologic conditions (*i.e.* location of direct flows) are key
301 drivers for cyanobacterial biomass and bloom development.
302
303 *Emerging cyanotoxins*
304 Many lake monitoring programs focus on the measurement of microcystins because of their vast
305 distribution (Loftin et al. 2016), ecotoxicity (Chorus and Bartram 1999), and relatively rapid
306 detection in whole water samples (*e.g.* ELISA). However, several studies using cyanobacterial
307 extracts have reported toxic effects that could not be explained solely by microcystin
308 concentration or presence, suggesting the possibility of other "toxic" compounds (Keil et al.
309 2002, Teneva et al. 2005, Baumann and Jüttner 2008, Smutná et al. 2014, Lenz et al. 2019).
310 Improved analytical techniques have identified numerous bioactive compounds such as
311 cyanopeptolins and anabaenopeptins that are readily detectable in freshwaters and often
312 produced simultaneously with microcystin variants (Harada et al. 1995, Welker and Von Döhren
313 2006, Gkelis et al. 2015, Beversdorf et al. 2017, 2018). In some cases, and consistent with our
314 results, anabaenopeptins are reported in equal or higher concentrations than microcystins
315 (Janssen 2019). For example, Beversdorf *et al.* (2017) reported an average of 0.65 µg/L total
316 microcystin in Lake Koshkonong, Wisconsin, while anabaenopeptin-B and -F were measured at
317 6.56 µg/L combined. Though there are no case studies of human toxicity caused by
318 anabaenopeptins, the compound inhibits carboxypeptidase A, and like microcystin, also inhibits

319 protein phosphatases with slightly overlapping inhibitory concentration ranges (Honkanen et al.
320 1990, Sano et al. 2001, Spoof et al. 2016). At present, the concentration to which
321 anabaenopeptins and other metabolites would have to reach to affect human health is currently
322 unknown resulting in a lack of regulations or advisories for recreational or drinking water.
323 However, a recent study by Lenz *et al.* (2019) reported induced toxicity by low concentrations
324 (10 µg/L) of anabaenopeptins, including AP-A, on *Caenorhabditis elegans* resulting in reduced
325 reproduction, reduced lifespan, and delayed hatching. Though compounds like AP-A have been
326 previously considered non-toxic, they may now represent a new class of emerging toxins, whose
327 potential impacts to human health and toxicity to aquatic organisms require immediate attention
328 and therefore, inclusion in risk assessment for lake mitigation and monitoring programs
329
330 *Recommendations for management*
331 Managers at the GRCA are interested in developing mitigation strategies for cyanobacterial
332 blooms because of the reservoir's functionality. Our results suggest these strategies will need to
333 be responsive to climate change with different short-term and long-term targets for nutrient loads
334 and water flow, which will fundamentally make management strategies to help address bloom
335 risks in Conestogo Lake challenging. Since Conestogo Lake operates with flood control and
336 base-flow augmentation as primary deliverables, changing the flow dynamics to mitigate
337 cyanobacterial biomass is not likely a feasible short-term or long-term option unless winter
338 storage volumes increase with the predicted increases in winter precipitation (McDermid et al.
339 2015). This, however, will have cumulative impacts on external P loads during the spring fill and
340 potentially drive earlier onset blooms if warmer conditions also accompany the precipitation.
341 Typically, the highest concentrations of external P accumulate in the reservoir during the spring

342 fill and then gradually decline throughout the course of the summer (Grand River Conservation
343 Authority 2018).

344 External P loading, as was one of the main drivers for the early 2017 event, will
345 likely only be of consequence if spring precipitation increases and/or
346 precipitation/drought cycles intensify during the summer drawdown period. Long-term
347 management goals may need to strive for incorporating watershed-wide regulation and
348 more local mitigation efforts. Because the catchment soil type is highly susceptible
349 erosion (Macrae et al. 2007, Grand River Conservation Authority 2018), increasing the
350 riparian zone surrounding the reservoir and in the upper reach of the Conestogo River
351 may reduce particulate P from entering the water column as has been demonstrated in
352 various other systems (Aguiar et al. 2015). At present, only a small strip of forested land
353 surrounds the main body of the reservoir, hence reduction of localized inputs may be
354 achievable, even if riverine inputs are more difficult to control.

355 While external inputs are important, hypolimnetic release of P from anoxic
356 sediments after the bloom onset was also observed during the 2017 sampling campaign.
357 At present, there is not sufficient evidence to conclude if sedimentary P release affected
358 cyanobacterial dominance and therefore, further work will be needed to determine
359 whether internal P release is a driver for the typically reported late August or early
360 September succession and dominance by cyanobacteria. However, if internal loading is a
361 key driver, numerous protocols to prevent or reduce the development of an anoxic
362 hypolimnion or removal of P rich sediments (such as through dredging or chemical
363 binding; Lürling & Faassen 2012) may be possible solutions for short-term control.
364 Unfortunately, the solution for mitigating cyanobacterial blooms is challenging and will

365 require an adaptive framework that incorporates physiochemical lake structure, biological
366 conditions, and climatic predictions. Thus, developing plans that incorporate site-specific
367 drivers with various climate models will help identify if and when managers need to intercede
368 with health risk notifications.
369

370 ## *Acknowledgments*

371 Funding for this work was provided by the Canada First Research Excellence Fund program.
372 This was a part of the Global Water Futures Initiative FORMBLOOM: FORecasting tools and
373 Mitigation options for diverse BLOOM-affected lakes as well as the ATRAPP project (Algal
374 Blooms, Treatment, Risk Assessment, Prediction and Prevention through Genomics) with from
375 Genome Canada and Genome Quebec. We thank S. Cooke, D. McFadden, and the Grand River
376 Conservation Authority for their cooperation and knowledgeable insight, R. Elgood, E. McQuay,
377 T. Cornell, and M. Soares-Paquin for assistance with sample collection and analysis, J. Atkins
378 for her GIS assistance, and the members of the Venkiteswaran and Schiff lab groups for their
379 reviews of manuscript drafts and friendly discussion.
380

381 ## *Data availability statement*

382 Data and code that support the analysis and findings in this study are available in figshare at
383 http://doi/10.6084/m9.figshare.7811963.

Literature Cited

Aguiar, T. R., K. Rasera, L. M. Parron, A. G. Brito, and M. T. Ferreira. 2015. Nutrient removal effectiveness by riparian buffer zones in rural temperate watersheds: The impact of no-till crops practices. Agricultural Water Management 149:74–80.

Allen, M. R., and W. J. Ingram. 2002. Constraints on future changes in climate and the hydrologic cycle. Nature 419:224–232.

Backer, L. C., S. V. McNeel, T. Barber, B. Kirkpatrick, C. Williams, M. Irvin, Y. Zhou, T. B. Johnson, K. Nierenberg, M. Aubel, R. LePrell, A. Chapman, A. Foss, S. Corum, V. R. Hill, S. M. Kieszak, and Y. S. Cheng. 2010. Recreational exposure to microcystins during algal blooms in two California lakes. Toxicon 55:909–921.

Baumann, H. I., and F. Jüttner. 2008. Inter-annual stability of oligopeptide patterns of Planktothrix rubescens blooms and mass mortality of Daphnia in Lake Hallwilersee. Limnologica 38:350–359.

Beversdorf, L. J., K. Rude, C. A. Weirich, S. L. Bartlett, M. Seaman, C. Kozik, P. Biese, T. Gosz, M. Suha, C. Stempa, C. Shaw, C. Hedman, J. J. Piatt, and T. R. Miller. 2018. Analysis of cyanobacterial metabolites in surface and raw drinking waters reveals more than microcystin. Water Research 140:280–290.

Beversdorf, L. J., C. A. Weirich, S. L. Bartlett, and T. R. Miller. 2017. Variable cyanobacterial toxin and metabolite profiles across six eutrophic lakes of differing physiochemical characteristics. Toxins 9.

Bouvy, M., S. M. Nascimento, R. J. R. Molica, A. Ferreira, V. Huszar, and S. M. F. O. Azevedo. 2003. Limnological features in Tapacurá reservoir (northeast Brazil) during a severe

406 drought. Hydrobiologia 493:115–130.

407 Bullerjahn, G. S., R. M. McKay, T. W. Davis, D. B. Baker, G. L. Boyer, L. V. D'Anglada, G. J.
408 Doucette, J. C. Ho, E. G. Irwin, C. L. Kling, R. M. Kudela, R. Kurmayer, A. M. Michalak,
409 J. D. Ortiz, T. G. Otten, H. W. Paerl, B. Qin, B. L. Sohngen, R. P. Stumpf, P. M. Visser, and
410 S. W. Wilhelm. 2016. Global solutions to regional problems: Collecting global expertise to
411 address the problem of harmful cyanobacterial blooms. A Lake Erie case study. Harmful
412 Algae 54:223–238.

413 Carmichael, W. W. 1997. The Cyanotoxins. Advances in Botanical Research 27:211–256.

414 Carmichael, W. W. 2001. Health Effects of Toxin-Producing Cyanobacteria: "The
415 CyanoHABs." Human and Ecological Risk Assessment: An International Journal 7:1393–
416 1407.

417 Carmichael, W. W., S. M. F. O. Azevedo, J. S. An, R. J. R. Molica, E. M. Jochimsen, S. Lau, K.
418 L. Rinehart, G. R. Shaw, and G. K. Eaglesham. 2001. Human fatalities form cyanobacteria:
419 Chemical and biological evidence for cyanotoxins. Page Environmental Health
420 Perspectives.

421 Chorus, I., and J. Bartram, editors. 1999. Introduction. Page Toxic Cyanobacteria in Water: a
422 guide to their public health consequences, monitoring and management. E & FN Spon,
423 London and New York.

424 Chorus, I., I. R. Falconer, H. J. Salas, and J. Bartram. 2000. Health Risks Caused By Freshwater
425 Cyanobacteria in Recreational Waters. Journal of Toxicology and Environmental Health,
426 Part B 3:323–347.

427 Codd, G. A. 2000. Cyanobacterial toxins, the perception of water quality, and the prioritisation
428 of eutrophication control. Ecological Engineering 16:51–60.

429 Fayad, P. B., A. Roy-Lachapelle, S. V. Duy, M. Prévost, and S. Sauvé. 2015. On-line solid-phase
430 extraction coupled to liquid chromatography tandem mass spectrometry for the analysis of
431 cyanotoxins in algal blooms. Toxicon 108:167–175.

432 Findlay, D. . L., and H. J. Kling. 2003. Protocols for measuring biodiversity: phytoplankton in
433 freshwater. Winnipeg: Department of Fisheries and Oceans.

434 Finley, A., S. Banerjee, and Ø. Hjelle. 2017. MBA: Multilevel B-Spline Approximation.

435 Gkelis, S., T. Lanaras, K. Sivonen, and O. Taglialatela-Scafati. 2015. Cyanobacterial toxic and
436 bioactive peptides in freshwater bodies of Greece: Concentrations, occurrence patterns, and
437 implications for human health. Marine Drugs 13:6319–6335.

438 Grand River Conservation Authority. 2018. Belwood and Conestogo Water Management
439 Reservoirs : An Assessment of Surface and Groundwater Conditions DRAFT January 2018.

440 Harada, K., K. Fujii, T. Shimada, M. Suzuki, H. Sano, K. Adachi, and W. W. Carmichael. 1995.
441 Two cyclic peptides, anabaenopeptins, a third group of bioactive compounds from the
442 cyanobacterium *Anabaena flos-aquae* NRC 525-17. Tetrahedron Letters 36:1511–1514.

443 Honkanen, R. E., J. Zwiller, R. E. Mooren, S. L. Daily, B. S. Khatra, M. Dukelow, and A. L.
444 Boynton. 1990. Characterization of Microcystin- LR, a potent inhibitor of type 1 and type
445 2A protein phosphatases. Journal of Biological Chemistry 265:19401–19404.

446 IPCC. 2007. Climate Change 2007: The Scientific Basis. Contribution of Working Group I to the
447 Fourth Assessment report of the Intergovernmental Panel on Climate Change. New York,

448 NY, USA.

449 Jacobsen, B. A., and P. Simonsen. 1993. Disturbance events affecting phytoplankton biomass,
450 composition and species diversity in a shallow, eutrophic, temperate lake. Page
451 Hydrobiologia.

452 Janssen, E. M.-L. 2019. Cyanobacterial peptides beyond microcystins – A review on co-
453 occurrence, toxicity, and challenges for risk assessment. Water Research 151:488–499.

454 Jöhnk, K. D., J. Huisman, J. Sharples, B. Sommeijer, P. M. Visser, and J. M. Strooms. 2008.
455 Summer heatwaves promote blooms of harmful cyanobacteria. Global Change Biology
456 14:495–512.

457 Jones, G. J., and W. Poplawski. 1998. Understanding and management of cyanobacterial blooms
458 in sub-tropical reservoirs of Queensland, Australia. Water Science and Technology 37:161–
459 168.

460 Keil, C., A. Forchert, J. Fastner, U. Szewzyk, W. Rotard, I. Chorus, and R. Krätke. 2002.
461 Toxicity and microcystin content of extracts from a Planktothrix bloom and two laboratory
462 strains. Water Research 36:2133–2139.

463 Lenz, K. A., T. R. Miller, and H. Ma. 2019. Anabaenopeptins and cyanopeptolins induce
464 systemic toxicity effects in a model organism the nematode *Caenorhabditis elegans*.
465 Chemosphere 214:60–69.

466 Loftin, K. A., J. L. Graham, E. D. Hilborn, S. C. Lehmann, M. T. Meyer, J. E. Dietze, and C. B.
467 Griffith. 2016. Cyanotoxins in inland lakes of the United States: Occurrence and potential
468 recreational health risks in the EPA National Lakes Assessment 2007. Harmful Algae

469 56:77–90.

470 Lürling, M., and E. J. Faassen. 2012. Controlling toxic cyanobacteria: Effects of dredging and
471 phosphorus-binding clay on cyanobacteria and microcystins. Water Research 46:1447–
472 1459.

473 Macrae, M. L., M. C. English, S. L. Schiff, and M. Stone. 2007. Intra-annual variability in the
474 contribution of tile drains to basin discharge and phosphorus export in a first-order
475 agricultural catchment. Agricultural Water Management 92:171–182.

476 McDermid, J., S. Fera, and A. Hogg. 2015. Climate change projections for Ontario: An updated
477 synthesis for policymakers and planners. Petersborough, Ontario.

478 Mitrovic, S. M., R. L. Oliver, C. Rees, L. C. Bowling, and R. T. Buckney. 2003. Critical flow
479 velocities for the growth and dominance of Anabaena circinalis in some turbid freshwater
480 rivers. Freshwater Biology 48:164–174.

481 Nauwerk, A. 1963. Die Beziehungen zwischen Zooplankton und Phytoplankton im See Erken.
482 Symbolae Botanicae Uppsaliensis 8:5–162.

483 O'Neil, J. M., T. W. Davis, M. A. Burford, and C. J. Gobler. 2012. The rise of harmful
484 cyanobacteria blooms: The potential roles of eutrophication and climate change. Harmful
485 Algae 14:313–334.

486 Okasanen, J., F. G. Blanchet, R. Kindt, P. Legendre, P. R. Minchin, R. B. O'hara, G. L. Simpson,
487 P. Solymos, M. H. H. Stevens, and H. Wagner. 2016. vegan: Community Ecology Package.

488 Paerl, H. W. 1988. Nuisance phytoplankton blooms in coastal, estuarine, and inland waters'.
489 Page Limnol. Oceanogr.

490 Paerl, H. W., W. S. Gardner, K. E. Havens, A. R. Joyner, M. J. McCarthy, S. E. Newell, B. Qin,
491 and J. T. Scott. 2016. Mitigating cyanobacterial harmful algal blooms in aquatic ecosystems
492 impacted by climate change and anthropogenic nutrients. Harmful Algae 54:213–222.

493 Paerl, H. W., and J. Huisman. 2009. Climate change: A catalyst for global expansion of harmful
494 cyanobacterial blooms. Environmental Microbiology Reports 1:27–37.

495 Paerl, H. W., and T. G. Otten. 2013. Harmful Cyanobacterial Blooms: Causes, Consequences,
496 and Controls. Microbial Ecology 65:995–1010.

497 Pinheiro, J., D. Bates, S. DebRoy, D. Sarkar, and R Core Team. 2018. {nlme}: Linear and
498 Nonlinear Mixed Effects Models.

499 Pouria, S., A. De Andrade, J. Barbosa, R. L. Cavalcanti, V. T. S. Barreto, C. J. Ward, W. Preiser,
500 G. K. Poon, G. H. Neild, and G. A. Codd. 1998. Fatal microcystin intoxication in
501 haemodialysis unit in Caruaru, Brazil. Lancet 352:21–26.

502 R Core Team. 2018. R: A Language and Environment for Statistical Computing. Vienna,
503 Austria.

504 Reichwaldt, E. S., and A. Ghadouani. 2012. Effects of rainfall patterns on toxic cyanobacterial
505 blooms in a changing climate: Between simplistic scenarios and complex dynamics. Water
506 Research 46:1372–1393.

507 Reynolds, C. S. 1984. Ecology of Freshwater Phytoplankton. Cambridge University Press.

508 Rott, E. 1981. Some results from phytoplankton counting intercalibrations. Schweizerische
509 Zeitschrift für Hydrologie 43:34–62.

510 Sano, T., T. Usui, K. Ueda, H. Osada, and K. Kaya. 2001. Isolation of new protein phosphatase

511 inhibitors from two cyanobacteria species, *Planktothrix* spp. Journal of Natural Products
512 64:1052–1055.

513 Smutná, M., P. Babica, S. Jarque, K. Hilscherová, B. Maršálek, M. Haeba, and L. Bláha. 2014.
514 Acute, chronic and reproductive toxicity of complex cyanobacterial blooms in *Daphnia*
515 *magna* and the role of microcystins. Toxicon 79:11–18.

516 Spoof, L., A. Błaszczyk, J. Meriluoto, M. Cegłowska, and H. Mazur-Marzec. 2016. Structures
517 and activity of new anabaenopeptins produced by Baltic Sea cyanobacteria. Marine Drugs
518 14:8.

519 Sukenik, A., A. Quesada, and N. Salmaso. 2015. Global expansion of toxic and non-toxic
520 cyanobacteria: effect on ecosystem functioning. Biodiversity and Conservation 24:889–908.

521 Teneva, I., B. Dzhambazov, L. Koleva, R. Mladenov, and K. Schirmer. 2005. Toxic potential of
522 five freshwater <i>Phormidium<\i> species (Cyanoprokaryota). Toxicon 45:711–725.

523 Vollenweider, R. A. 1968. Scientific fundamentals of the eutrophication of lakes and flowing
524 waters, with particular reference to nitrogen and phosphorus as factors in eutrophication.
525 Page Paris: Organisation for Economic Co-operation and Development. Technical Report
526 DAS/CS1/68.27.

527 Welker, M., and H. Von Döhren. 2006. Cyanobacterial peptides - Nature's own combinatorial
528 biosynthesis. FEMS Microbiology Reviews 30:530–563.

529 Wetzel, R. G. 2001. Limnology : lake and river ecosystems. Third. Academic Press, San Diego.

530 Winter, J. G., A. M. DeSellas, R. Fletcher, L. Heintsch, A. Morley, L. Nakamoto, and K. Utsumi.
531 2011. Algal blooms in Ontario, Canada: Increases in reports since 1994. Lake and Reservoir

532 Management 27:105–112.

533 Winter, J. G., E. T. Howell, and L. K. Nakamoto. 2012. Trends in nutrients, phytoplankton, and
534 chloride in nearshore waters of Lake Ontario: Synchrony and relationships with physical
535 conditions. Journal of Great Lakes Research 38:124–132.

536 Wood, S. A., H. Borges, J. Puddick, L. Biessy, J. Atalah, I. Hawes, D. R. Dietrich, and D. P.
537 Hamilton. 2017. Contrasting cyanobacterial communities and microcystin concentrations in
538 summers with extreme weather events: insights into potential effects of climate change.
539 Hydrobiologia 785:71–89.

540 Yakobowski, S. J. 2008. Ecological Factors Controlling Microcystin Concentrations in the Bay
541 of Quinte, Maumee Bay, and Three Grand River Reservoirs. University of Waterloo.

542

543

544 **Table 1.** Physical and chemical water column summary with mean (SD) [minimum – maximum]

545 across the sampling campaign at each site.

Site	NO_3-N (mg-N/L)	TDN (mg-N/L)	SRP (µg-P/L)	TDP (µg-P/L)	TP (µg-P/L)
Center	4.82 (0.59) [3.99 - 5.65]	5.32 (0.64) [4.24 - 5.86]	13.66 (22.86) [1.52 - 65.2]	26.41 (26.32) [9.96 - 85.77]	39.84 (27.59) [14.99 - 103.48]
East	4.37 (0.79) [3.34 - 5.63]	4.74 (0.89) [3.39 - 5.85]	5.89 (8.45) [1.56 - 24.61]	18.53 (11.14) [7.79 - 41.59]	49.54 (11.08) [35.2 - 68.65]
West	4.69 (0.57) [3.89 - 5.43]	5.1 (0.83) [3.94 - 6.03]	4.09 (4.73) [1.23 - 13.48]	15.99 (7.7) [8.37 - 29.83]	39.35 (4.26) [34.69 - 47.04]

546

547 **Table 2**. Quantified cyanobacterial metabolites across sampling sites as measured my LC-HMRS
548 with values which exceeded the limit of detection (LOQ) presented as mean ng/L (standard
549 deviation ng/L), those in italics exceeded the limit of detection (LOD) but not the limit of
550 detection (LOQ), and those with (-) < LOD. MC-LA, -LY, -LW, -LF, -HiIR, -HtyR, and CPA
551 were not detected in samples.

552
553

Date	Site	cyanobacterial secondary metabolites						
		AP-A	MC-LR	MC-RR	MC-YR	ATX	HATX	CYN
21 Jun	Center	-	-	-	-	-	-	-
05 Jul		-	-	-	*33.26 (16.08)*	-	-	-
14 Jul		*23.72 (4.89)*	-	-	*20.6 (29.13)*	-	-	-
18 Jul		109.25 (78.62)	406.88 (18.06)	-	-	-	-	-
25 Jul		189.65 (35.58)	88.18 (6.22)	*35.47 (9.17)*	*19.95 (28.21)*	-	-	-
01 Aug		278.84 (27.42)	16.77 (10.62)	-	59.22 (16.5)	-	-	-
10 Aug		619.33 (140.95)	-	-	*19.41 (1.29)*	-	-	-
17 Aug		343.99 (50.32)	-	-	-	-	-	-
05 Jul	East	-	-	-	-	-	-	-
11 Jul		*18.59 (26.29)*	-	-	-	-	-	-
19 Jul		-	763.25 (154.17)	120.97 (1.56)	97.26 (36.16)	-	-	-
25 Jul		174.25 (34.91)	72.07 (23.34)	*27.59 (2.67)*	-	-	-	-
31 Jul		188.58 (108.52)	-	-	-	-	-	-
10 Aug		411 (30.56)	-	-	-	-	-	-
17 Aug		856.77 (37.15)	-	-	-	-	-	-
11 Jul	West	51 (24.31)	-	-	-	-	-	-
19 Jul		160.79 (14.53)	211.23 (23.56)	-	-	-	-	-
25 Jul		33.89 (25.24)	106.53 (28.81)	*30.03 (8.44)*	-	-	-	-
31 Jul		242.35 (29.74)	-	-	-	-	-	-
10 Aug		471.57 (75.91)	-	-	*26.43 (37.38)*	-	-	-
17 Aug		846.72 (0.53)	-	-	-	-	-	-

Abbreviations: anabaenopeptin A (AP-A), microcystin (MC-), anatoxin (ATX), homoanatoxin-a (HATX), cylindrospermopsin (CYN), cyanopeptolin-a (CPA)

554

555 **Figure legends**

556 **Figure 1**. Watershed and bathymetric (*a*) map of Conestogo Lake, Mapleton Township, Ontario
557 with sampling sites for the west arm (CLW), center (CLC), and east arm (CLE) of the reservoir.
558 Bathymetric data is scaled to the maximum dam stage elevation (meters at sea level; m.a.s.l.).
559 Total precipitation in the Upper Conestogo watershed (*b*, gauge in Arthur, ON) is directly related
560 to the mean daily flow rate (*c*) into the east arm (gauges in Drayton and Moorefield, ON) and the
561 calculated residence time (*d*) in the reservoir. Average flow rate (red line, *c*) is typically near
562 0.01 m/s. An intense rainfall event on 23-24 Jun (grey vertical bar) resulted in a notable increase
563 in the mean daily storage volume (1000 m^3) of the reservoir (*e*). Dark gray bars represent
564 standard deviation. This figure contains information made available under GRCA's Open Data
565 Licence v3.0 (panel a) and v2.0 (panels *b* - *e*).
566
567 **Figure 2.** Nutrient profiles for phosphorus (*a*; P, µg-P/L) and nitrogen species (*b*; N, mg-N/L)
568 collected at 2, 7, and 0.5m from the bottom at each of the sampling locations. The flood event
569 (white vertical bar) introduced increased levels of all measured P species but did not greatly
570 affect N species (see Figure S1). The dynamic area of the colored box reflects the changing
571 depths within each sample location. Profile depths at each site were standardized to the dam
572 stage elevation (m) at the time of sampling and illustrate both the differences in bottom depth
573 and reservoir drawdown during the sampling campaign.
574
575 **Figure 3.** Cyanobacterial biomass (*a*) and cyanotoxin concentration trends < LOQ for
576 anabaenopeptin-A (AP.A) and microcystin-LR (MC.LR), -YR (MC.YR), and -RR (MC.RR) (*b*)
577 in each of the three sampling locations (*l* to *r:* West, Center, and East) were detected

578 approximately 2 weeks following the flood event on 23-24 Jun (DOY 172; grey vertical bar).
579 *Aphanizomenon flos-aquae* dominated (> 50%) phytoplankton biomass in the west and east arms
580 of Conestogo Lake near 10 Jul 2017 (DOY 191) and in the center near 16 Jul 2017 (DOY 197).
581 The bloom period lasted between 26-34 days depending on the sampling site with a site-specific
582 peak bloom biomass occurring near 25 Jul 2017 (DOY 206). Of the seven cyanobacterial species
583 detected in Conestogo Lake, various strains of *A. flos-aquae*, *D. flos-aquae* (*Anabaena flos-*
584 *aquae*), *M. aeruginosa*, and *W. compacta* have been documented as potential toxin producers.
585

586 **Figure 1**

587

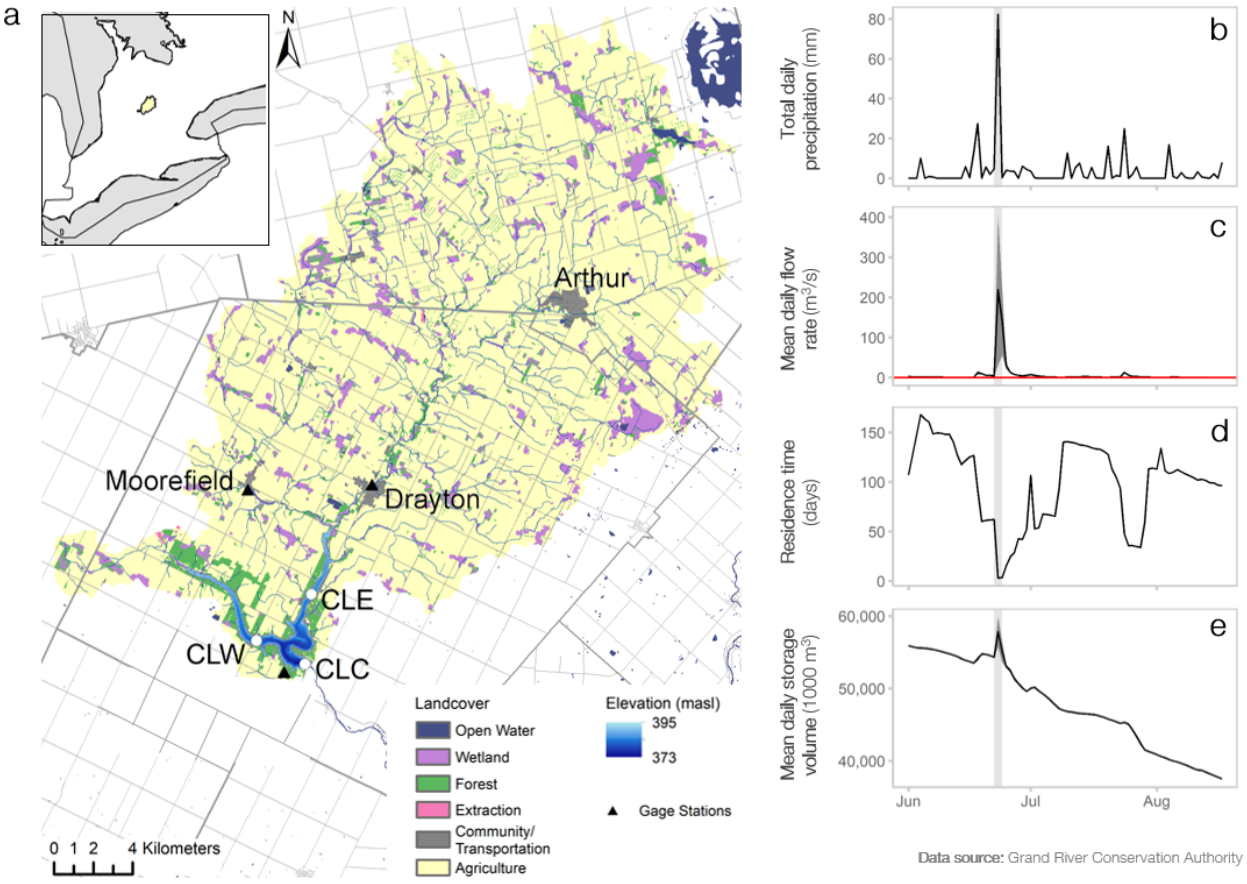

588

589 **Figure 2**

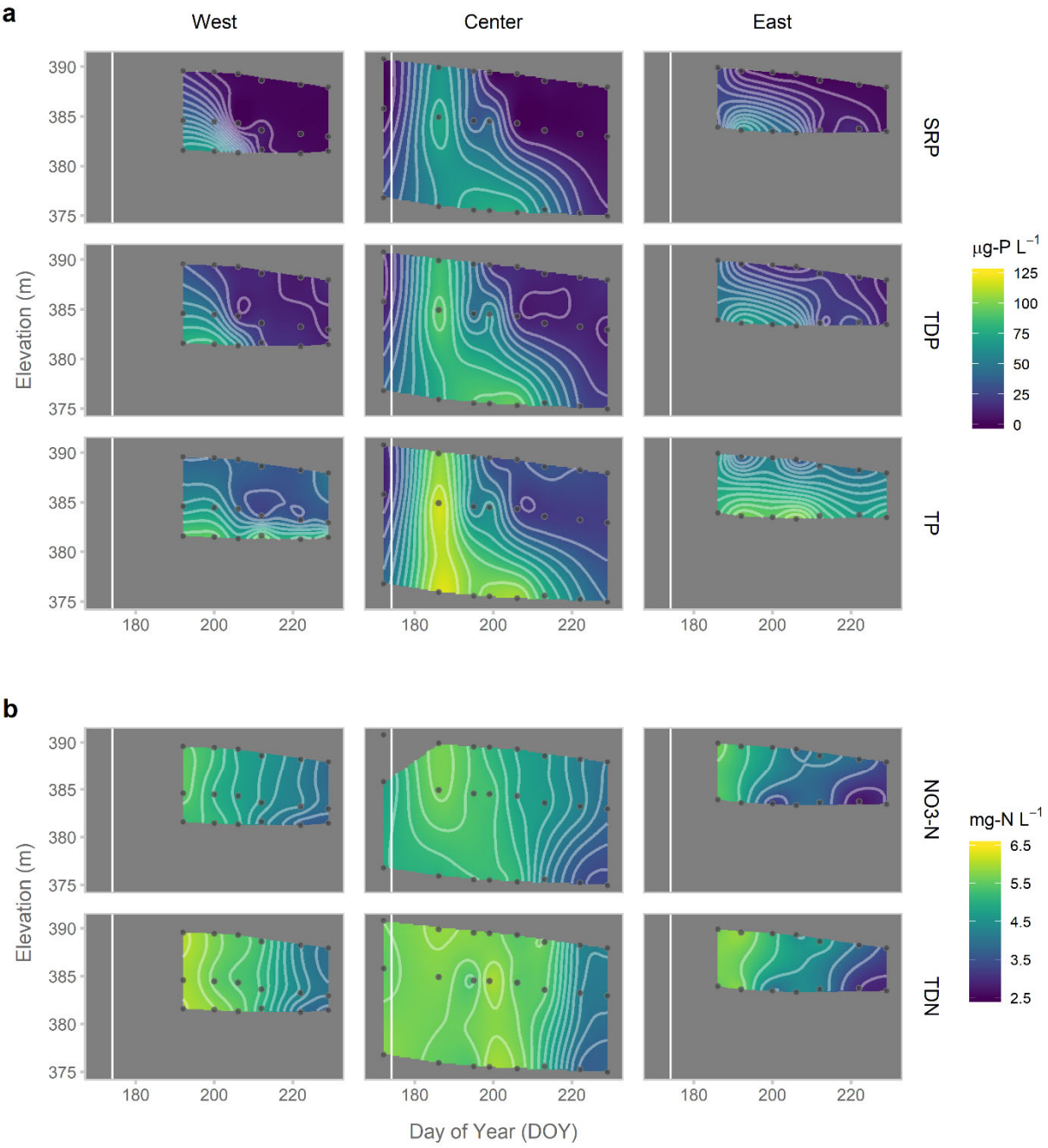

590

591 **Figure 3**
592

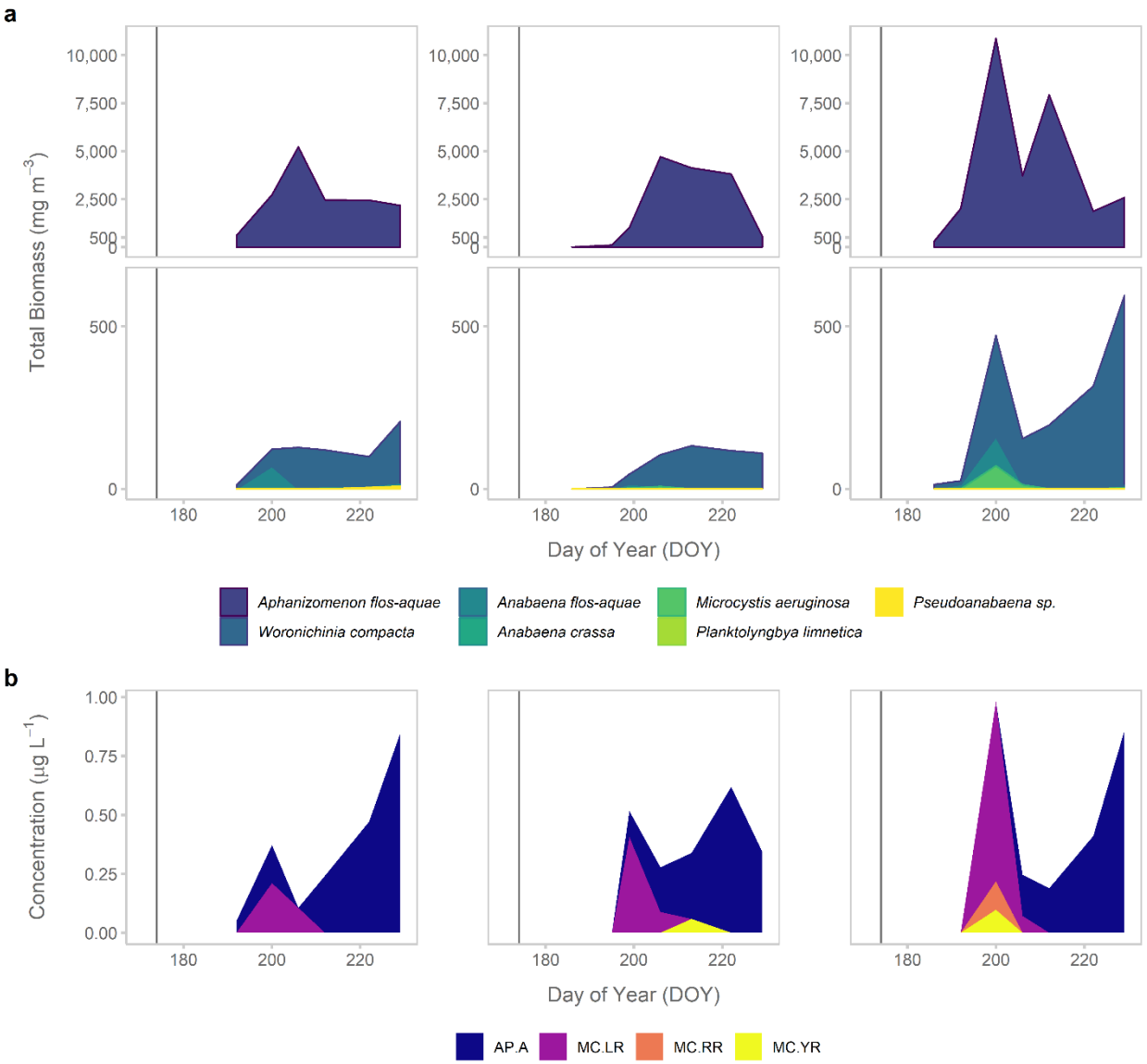

593